Inorganic Chemistry

Article

pubs.acs.org/IC

Systematic Investigation of Zinc Aminoalkylphosphonates: Influence of the Alkyl Chain Lengths on the Structure Formation

Corinna Schmidt and Norbert Stock*

Institut für Anorganische Chemie, Christian-Albrechts-Universität, Max-Eyth Strasse 2, D 24118 Kiel, Germany

Supporting Information

ABSTRACT: With the high-throughput (HT) methodology, the bifunctional aminoalkylphosphonic acids (AAPA) linker molecules 2-aminoethyl- (AEPA), 3-aminopropyl- (APPA), and 4-aminobutylphosphonic acid (ABPA) [$HO_3P{-}C_nH_{2n}{-}NH_2$ (n = 2−4)] and zinc nitrate were used to synthesize new metal phosphonates in order to investigate the influence of the alkyl chain length on the structure formation. The systematic investigations led to one known ($ZnO_3PC_2H_4NH_2$) and six new compounds: one using AEPA, three using APPA, and two using ABPA. The crystal structures of five compounds were determined by single crystal X-ray diffraction, using X-ray powder diffraction (XRPD) data as well as structure modeling employing force field methods. For compound **1**, $Zn(O_3P{-}C_2H_4{-}NH_3)(NO_3)(H_2O)$ (monoclinic, Cc, a = 4.799(1) Å, b = 29.342(6) Å, c = 5.631(1) Å, β = 91.59(3)°, V = 792.7(3) Å^3, Z = 4), and compound **2**, $Zn_2(OH)(O_3P{-}C_3H_6{-}NH_3)(NO_3)$ (monoclinic, $P2/c$, a = 12.158(2) Å, b = 5.0315(10) Å, c = 13.952(3) Å, β = 113.23(3)°, V = 784.3(3) Å^3, Z = 2), the structures were determined using single crystal X-ray diffraction data. The crystal structures of $[Zn(O_3P{-}C_3H_6{-}NH_2)]{\cdot}H_2O$ (**3**) (monoclinic, $P2_1/c$, a = 9.094(2) Å, b = 5.0118(7) Å, c = 16.067(4) Å, β = 90.38(2)°, V = 732.3(2) Å^3, Z = 4) and $Zn(O_3P{-}C_4H_8{-}NH_2)$ (**5**) (monoclinic, $P2_1/c$, a = 8.570(7) Å, b = 8.378(4) Å, c = 9.902(6) Å, β = 90.94(5)°, V = 710.9(8) Å^3, Z = 4) were determined using XRPD data. The structural model for compound **6**, $Zn(O_3P{-}C_4H_8{-}NH_3)(NO_3)(H_2O)$, was established using lattice parameters from XRPD data and following crystal structure modeling employing force field methods. The structures depend strongly on the alkyl chain length n. For n = 2 and 4 isoreticular compounds are observed, while n = 3 leads to new structures. Larger amounts of all compounds were obtained employing scale-up syntheses in a conventional oven as well as in a microwave reactor system. In addition, in situ energy dispersive X-ray diffraction (EDXRD) experiments at 130 °C were performed at beamline F3 at HASYLAB, DESY, Hamburg, to investigate the formation of compounds **2** and **3** as well as the phase transformation of **2** into **3** upon addition of NaOH. All compounds were characterized in detail using X-ray powder diffraction, IR/Raman spectroscopy, and thermogravimetric and elemental analysis.

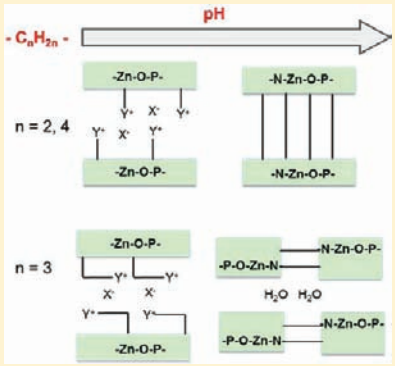

INTRODUCTION

The interest in inorganic−organic hybrid compounds has gained increased attention in recent years due to their immense structural diversity as well as their potential applications, for example, in catalysis or gas or charge storage.[1−3] Mostly metal polyphosphonates,[4−6] -carboxylates,[7] and -sulfonates[5] have been investigated, but multivalent linker molecules containing two or more different functional groups have been applied less frequently. Regarding metal phosphonates, most of these compounds contain phosphonocarboxylate,[8−10] phosphonosulfonate,[11−13] as well as aminophosphonate ions.[14,15] Few previous studies have shown that the length of the organic unit ($-C_nH_{2n}-$) has a strong influence on the structure formation. Thus, Mallouk et al. reported a homologous series of divalent layered metal phosphonates [$(M(O_3PC_nH_{2n+1}){\cdot}H_2O$ (M = Mg, Mn, Zn; n = 1−12)]. The increase of the linker length led to isoreticular structures where the interlayer spacing varies according to the length of the alkyl group.[16] The same group reported a series of calcium alkylphosphonates employing phosphonic acids $H_2O_3PC_nH_{2n+1}$, n = 1−18.[17] For n = 1−5 metal phosphonates $Ca(O_3PC_nH_{2n+1})$ are formed while for n > 5 metal hydrogenphosphonates $Ca(HO_3PC_nH_{2n+1})_2$ are observed. These systematic studies were extended to diphosphonic acids $(H_2O_3P(CH_2)_nPO_3H_2)$ (n = 2−9) using vanadium as the metal.[18] Three different structures are observed for n = 2−5, 6−8, and 9, respectively. Recently, the investigations were further extended to the chemistry of phosphonoalkylsulfonic acids $(HO_3SC_nH_{2n}PO_3H_2)$ (n = 2, 4).[19]

With a comparison of primary aminophosphonic acids ($H_2O_3P{-}C_nH_{2n}{-}NH_2$) to other difunctionalized linker molecules, these have been used less frequently for the synthesis of hybrid compounds. While mostly 2-aminoethylphosphonic acid in combination with divalent metal ions Zn^{2+},[14] Cd^{2+},[20] Cu^{2+},[21] Cr^{2+},[22] and Co^{2+}[23] have been reported, the number of metal 3-aminopropylphosphonates is by far smaller.[24,25] Furthermore, metal aminomethylphosphonates (M = Zn^{2+}, Cd^{2+}, Pb^{2+}, Hg^{2+}, Ag^{+}) have been described.[26] A list of the known metal aminoethyl- and aminopropylphosphonates is given in Table S1. These hybrid compounds crystallize in layered

Received: December 1, 2011
Published: February 10, 2012

   dx.doi.org/10.1021/ic202589s | *Inorg. Chem.* 2012, 51, 3108−3118

and pillared layered structures. While the phosphonate oxygen atoms connect the metal ions at all times, the role of the amino function is variable. It can coordinate to the metal ion, or it is protonated and protrudes into the interlayer space. In case of a protonated amino group, chloride- or sulfate ions are located between the layers and are involved in hydrogen bonding.[25] The coordination of the amino group to the metal ion leads in some cases to pillared-layered structures.[20]

Here, we present the optimized synthesis of the aminoalkylphosphonic acids (AAPA) 2-aminoethylphosphonic acid (AEPA) ($H_2O_3P-C_2H_4-NH_2$), 3-aminopropylphosphonic acid (APPA) ($H_2O_3P-C_3H_6-NH_2$), and 4-aminobutylphosphonic acid (ABPA) ($H_2O_3P-C_4H_8-NH_2$) and the systematic investigation of the systems $Zn^{2+}/(H_2O_3P-C_nH_{2n}-NH_2)/H_2O/NaOH$ (n = 2−4) applying our high-throughput (HT) methodology.[27] This methodology allows the systematic exploration of multiparameter fields in order to study the influence of parameters, such as the pH-value,[28] the reaction temperature,[29] or the molar ratio of the reactants on the product formation.[30] It allows us to rapidly discover new compounds and to establish reaction trends. Since this method gives no information about the crystallization, in situ EDXRD measurements were also performed[31,32] for the formation of **2** and **3** as well as the conversion of **2** into **3**.

EXPERIMENTAL SECTION

The syntheses of the linker molecules were performed on the basis of reported procedures, but several steps were optimized. All reagents and solvents were purchased from commercial sources. They were of analytical grade and were used as obtained except triethyl- and diethylphosphite, which were distilled for purification. The reaction schemes for the syntheses of the linker molecules are shown in Scheme S1−S3 in the Supporting Information. HT-X-ray powder diffraction (XRPD) measurements were performed on a Stoe Stadi P HT-diffractometer in transmission geometry with Cu Kα1 radiation, equipped with an image plate detector. MIR spectra were collected on a Bruker Alpha spectrometer equipped with a diamond ATR unit in the spectral range 4000−400 cm^{-1}. Raman spectra were recorded using a Bruker FRA 106 Raman spectrometer. The thermogravimetric (TG) analyses were executed with a NETSCH STA 409 CD analyzer, under air (75 mL/min), with a heating rate of 2 K/min. Elemental analyses were carried out using a Eurovektor EuroEA elemental analyzer. ^1H, ^{13}C, and ^{31}P NMR spectroscopy was performed on a BRUKER ARX300 spectrometer. The in situ EDXRD measurements were executed at beamline F3 at HASYLAB, DESY, Hamburg.

Synthesis of 2-Aminoethylphosphonic Acid (AEPA). The three step reaction started with a solution of acrylamide and diethylphosphite in a molar ratio of 1:1.1 (Scheme S1). A mixture of 7.82 g (0.11 mol) of acrylamide (**I**) and 12.9 mL (0.1 mol) of diethyl phosphite (**II**) was heated to 35 °C until a clear solution was formed. A 1 mL portion of a 3 mol/L sodium ethanolate solution (0.35 g Na in 5 mL EtOH) was added slowly to the cooled reaction mixture (0 °C). The beginning of the reaction was observed by an increase of the reaction temperature. The reaction mixture was kept for 2 days without stirring at room temperature.[33] After the mixture cooled to to 0 °C and was scratched with a glass bar at the flask wall, the crude product crystallized. The crude product was recrystallized in toluene, and 2-diethylphosphonatocarbamoyl (**III**) was obtained (yield: 48 mmol, 48%).[34] A 4 g (19.12 mmol) portion of **III** and 6.77 g (21.03 mmol) of (diacetoxyiodo)benzene (**IV**) were dissolved in a mixture of acetonitrile (45 mL)/acetic acid (6 mL, 99%)/water (15 mL) and stirred at room temperature for 1 day. After vacuum evaporation of the solvent, the crude 2-aminoethylphosphonic acid dithylester (**V**) was washed three times with water (yield: 13.0 mmol, 68%). A 0.94 g (5.19 mmol) portion of **V** was dissolved in 200 mL of 6 mol/L hydrochloric acid and refluxed for 2 days. After evaporation of the solvent and washing three times with water/ethanol (1:1), the hydrochloride salt of AEPA was dissolved in ethanol. Addition of 2 mL of propylene oxide led to the crystallization of the crude acid **VI**. The crude product was recrystallized in water/ethanol (1:3) (yield: 2.69 mmol, 52%).[35] ^1H NMR (D_2O): δ = 1.85 (m, 2H, $-CH_2-P$), 3.09 (m, 2H, $-CH_2-N$) ppm. ^{13}C NMR (D_2O): δ = 26.09 (d, $^1J_{C,P}$ = 132.2 Hz, $-CH_2-P$), 35.48 (s, $-CH_2-N$) ppm. ^{31}P NMR: δ = 19.81 (s) ppm.

Synthesis of 3-Aminopropylphosphonic Acid (APPA). The 3-aminopropylphosphonic acid was synthesized in a three step reaction (Scheme S2). At first, 10 g (37.3 mmol) of *N*-(3-bromopropyl)-phthalimide (**VII**) was dissolved at room temperature in 25.5 mL (149 mmol) of triethyl phosphite (**VIII**), and the reaction mixture was refluxed for 24 h. Excess of triethylphosphite was removed under vacuum, and 3-[(phthalimido)propyl]phosphonic acid diethylester (**IX**) was obtained (yield: 27.3 mmol, 73%). A 7.65 g (26.1 mmol) portion of **IX** was dissolved in 200 mL of ethanol, and 3.5 mL of an 80% hydrazine solution in H_2O was added. The reaction mixture was stirred at room temperature for 72 h. Afterward, phthalhydrazide was filtered off, the solvent was evaporated, and 3-aminopropylphosphonic acid diethylester (**X**) was obtained (yield: 9.66 mmol, 37%).[36] A 1.8 g (9.22 mmol) portion of **X** was dissolved in 200 mL of 6 mol/L hydrochloric acid and refluxed for 2 days. After evaporation of the solvent and washing three times with water/ethanol (1:1), the hydrochloride salt of APPA was dissolved in ethanol. Addition of 2 mL of propylene oxide led to the crystallization of the crude acid **XI**. The crude product was recrystallized in water/ethanol (1:3) (yield: 3.96 mmol, 43%).[35] ^1H NMR (D_2O): δ = 1.55 (m, 2H, $-CH_2-P$), 1.77 (m, 2H, $-CH_2-$), 2.95 (m, 2H, $-CH_2-$) ppm. ^{13}C NMR (D_2O): δ = 40.17 (d, $^3J_{C,P}$ = 17.6, $-CH_2-N$), 24.9 (d, $^1J_{C,P}$ = 134.7 Hz, $-CH_2-P$), 21.41 (d, $^2J_{C,P}$ = 4.1 Hz, $-CH_2-$) ppm. ^{31}P NMR: δ = 24.36 (s) ppm.

Synthesis of 4-Aminobutylphosphonic Acid (ABPA). ABPA was synthesized in a four step reaction (Scheme S3). At first 36 mL (300 mmol) of 1,4-dibromobutane (**XII**) was dissolved in 600 mL of acetone and heated up to 56 °C. A 22.8 g (123 mmol) portion of potassium phthalimide (**XIII**) was added over a period of 3.5 h, and the reaction mixture was refluxed for 24 h. The crude product was filtered off and recrystallized in toluene to yield *N*-(4-bromobutyl)-phthalimide (**XIV**) (yield: 76.2 mmol, 62%).[37] A 21.5 g (76.2 mmol) portion of **XIV** was added at room temperature to 65.4 mL (381 mmol) of triethyl phosphite and refluxed for 21 h. An excess of triethyl phosphite was removed by vacuum distillation, and 4-[(phthalimido)-butyl]phosphonic acid diethylester (**XV**) was obtained (yield: 59.4 mmol, 78%). A mixture of 20.2 g (59.4 mmol) of **XV**, 400 mL of ethanol, and 17 mL of a 80% hydrazine solution was stirred at room temperature for 72 h. Afterward, phthalhydrazide was filtered off, and the liquid phase was evaporated to obtain 4-aminobutylphosphonic acid diethylester (**XVI**) (yield: 27.2 mmol,46%).[36] A 5 g (23.9 mmol) portion of **XVI** was dissolved in 100 mL of diethyl ether, and 10.8 mL (95.6 mmol) of bromotrimethylsilane (**XVII**) was added slowly. The reaction mixture was stirred at room temperature for 12 h, and 20 mL of methanol was added. The methanolic phase was isolated, and the solvent was evaporated.[38] The crude 4-aminobutylphosphonic acid (**XVIII**) was recrystallized in ethanol (yield: 8.36 mmol, 35%). ^1H NMR (D_2O): δ = 2.92 (t, 2H, $^3J_{H,H}$ $-CH_2-$), 1.62 (m, 6H, $-CH_2-CH_2-CH_2-P$) ppm. ^{13}C NMR (D_2O): δ = 19.67 (d, $^2J_{C,P}$ = 4.4 Hz, $-CH_2-$), 26.13 (d, $^1J_{C,P}$ = 135.2 Hz, $-CH_2-P$), 27.83 (d, $^3J_{C,P}$ = 16.9 Hz, $-CH_2-$), 39.25 (s, $-CH_2-N$) ppm. ^{31}P NMR: δ = 30.91 (s) ppm.

HT Experiments. With our HT method the systems $Zn(NO_3)_2\cdot 6H_2O$/AAPA/NaOH/H_2O were investigated under hydrothermal conditions. All starting materials were applied as aqueous solutions. The reaction block was heated to 130 °C in 2 h. After 48 h at the reaction temperature the reactor block was allowed to cool down within 12 h. Custom made HT reactors were employed containing 48 PTFE vessels each with a maximum volume of 300 μL.[27] The molar ratios $Zn(NO_3)_2\cdot 6H_2O$/AAPA were varied from (0.17−6.5)/1. The amount of NaOH was varied from (0.17−6)/1 (NaOH/AAPA). The starting materials were added to the PTFE vessels in the following order: AAPA, $Zn(NO_3)_2\cdot 6H_2O$, H_2O, and NaOH. The reaction products were filtered off, washed with water, and dried in air. All samples were characterized by XRPD measurements. The

dx.doi.org/10.1021/ic202589s | Inorg. Chem. 2012, 51, 3108−3118

concentrations of the starting solutions and the exact amounts of the starting materials employed are given in Tables S2–S4 in the Supporting Information.

Scale-up Syntheses. Larger amounts of compounds **1**–**5** were synthesized in Schott Duran glass culture tubes (5 mL) by using the optimized reaction conditions established from the HT experiments (Table S5). All reactions were carried out at a temperature of 130 °C for 48 h. The reaction products were filtered off and washed with water. The purity of the products were confirmed by C,H,N analyses (Table S6).

Microwave-Assisted Synthesis. The use of microwave (MW)-assisted heating allows an acceleration of the reaction time as well as phase selectivity.[39] Compound **6** obtained from the HT synthesis exhibits an unknown impurity; therefore, MW-assisted heating was applied to obtain phase pure product of **6**. Crystalline samples of all compounds could be obtained by applying MW-assisted heating. Exactly the same amounts as used for the scale-up synthesis were used for the microwave experiments. The starting materials were mixed in a microwave tube (Biotage, 0.5–2 mL glass reactor) and sealed with a septum. The reaction mixture was homogenized by shaking and heated in a microwave oven (Biotage Injector) for 1 h at 130 °C under stirring. The products were isolated by filtration and washed with water. The product **6** obtained from the MW-assisted synthesis was used for the structure determination from XRPD data.

Structure Determination. Using a polarizing microscope, suitable crystals of the compounds $Zn(O_3P–C_2H_4–NH_3)(NO_3)(H_2O)$ (**1**) and $Zn_2(OH)(O_3P–C_3H_6–NH_3)_2(NO_3)$ (**2**) were carefully selected from the HT experiments. X-ray diffraction measurements were conducted on a STOE IPDS diffractometer equipped with a fine-focus sealed tube (Mo Kα radiation, λ = 71.073 pm). For data reduction and absorption correction the programs XRED and X-SHAPE were used.[40] The crystal structures were solved by direct methods with SIR2008[41] and SHELXS-97, for **1** and **2**, respectively, and refined with SHELXL-97.[42] For both compounds all hydrogen atoms of the $–CH_2–$ and $–NH_3^+$ groups were placed onto calculated positions. The hydrogen atoms of OW in compound **1** as well as the hydrogen atom of the hydroxyl group O4 in compound **2** were also placed onto calculated positions. Restraints were applied to all N–O distances of the nitrate ion in compound **1**. The comparison of the measured and the calculated XRPD patterns is shown in the Supporting Information (Figures S1 and S2). The XRPD measurements were performed on a STOE Stadi-P powder diffractometer in transmission geometry with Cu Kα1 radiation (λ = 154.0598 pm) equipped with a position-sensitive detector. The structure determination of $[Zn(O_3P–C_3H_6–NH_2)]\cdot H_2O$ (**3**) and $Zn(O_3P–C_4H_8–NH_2)$ (**5**) was accomplished using in-house XRPD data. Indexing of the XRPD patterns of **3** and **5** was done using the program EXPO2009,[43] and the cell parameters were refined applying the program WinXPOW[44] (FOM **3**, 25; FOM **5**, 29). Structure determinations were carried out with EXPO2009 using direct methods. All atoms were observed in the structure solution, and the atomic coordinates were set as the starting model for the Rietveld refinement applying the program TOPAS.[45] The Rietveld refinement involved the following parameters for compound **3**: 4 cell parameters, 30 atomic coordinates (Table S15), 1 overall thermal factor, 1 scale factor, 1 zero point, and 12 background parameters. For compound **5**, 4 cell parameters, 30 atomic coordinates (Table S16), 1 overall thermal factor, 1 scale factor, 1 zero point, and 11 background parameters were used for the Rietveld refinement. Preferred orientation was modeled using spherical harmonics series. Restrains were applied to the P – O, P – C, C – C and C – N lengths in both compounds and to the O – P – C and C – C – C angles of **5**. The results of the final Rietveld refinements are shown in Figure 6 and 9. The XRPD patterns of $Zn(O_3P–C_3H_6–NH_3)(NO_3)(H_2O)$ (**4**) and $Zn(O_3P–C_4H_8–NH_3)(NO_3)(H_2O)$ (**6**) were successfully indexed using synchrotron data for **4** (Figure S3, Table 2) and in-house XRPD data for **6** (Table 2). A Pawley fit was performed for **4** to confirm the phase purity and the indexed lattice parameters (Figure S3). While the structure determination of **4** was not possible until now, structural modeling using the program Materials Studio 5.0[46] was employed to extract a structural model of **6**. Thus, starting from the crystal structure of **1** ($Zn(O_3P–C_2H_4–NH_3)(NO_3)(H_2O)$) and the refined cell parameters of **6** ($Zn(O_3P–C_4H_8–NH_3)(NO_3)(H_2O)$), the alkyl chain was extended by two carbon atoms, and in analogy to the structure of **1** hydrogen bonds between the $–NH_3^+$ groups and the nitrate ions were set up. This model was submitted to a full energy minimization, including the geometry optimization, using the universal force field (UFF) as implemented in the Forcite module of Materials Studio 5.0. Structure refinement using the Rietveld method was not possible until now because of the low crystallinity of **6**. Nevertheless, the measured and the simulated XRPD patterns (Figure 12) agree well. Results of the crystallographic work are summarized in Tables 1 and 2.

Table 1. Summary of Crystal Data and Refined Structure Parameters for $Zn(O_3P–C_2H_4–NH_3)(NO_3)(H_2O)$ (1) and $Zn_2(OH)(O_3P–C_3H_6–NH_3)_2(NO_3)$ (2)

	compound **1**	compound **2**
formula	$C_2H_9O_7PN_2Zn$	$C_6H_{19}O_{10}P_2N_3Zn_2$
fw (g/mol)	269.46	485.94
cryst syst	monoclinic	monoclinic
space group	*Cc* (No. 9)	*P2/c* (No. 13)
a, *b*, *c* (Å)	4.799(1)	12.158(2)
	29.342(6)	5.0315(10)
	5.631(1)	13.952(3)
β (deg)	91.59(3)	113.23(3)
V (Å^3)	792.7(3)	784.3(3)
Z	4	2
total, unique data	3775, 1899	4538, 2073
R_{int}	0.043	0.048
obsd data [$I > 2\sigma(I)$]	1738	1684
R1, wR2 [$I > 2\sigma(I)$]	0.0457, 0.1069	0.0398, 0.1089
R1, wR2 [all data]	0.0522, 0.1097	0.0552, 0.1152
GOF	1.060	1.095
Flack parameter	0.028(23)	
Δe min/max (e/Å^3)	−0.63, 1.64	−0.55, 0.70

Table S17 contains the atomic coordinates of the structural model of **6**. Crystallographic data (excluding structure factors) for the structures in this paper have been deposited with the Cambridge Crystallographic Data Centre as supplementary publication nos. CCDC-854343, 854345, 845342, 854344 for **1**, **2**, **3**, and **5**, respectively. Copies of the data can be obtained, free of charge, on application to CCDC, 12 Union Road, Cambridge CB2 1EZ, U.K. (fax +44 1223 336033 or email deposit@ccdc.cam.ac.uk).

In Situ Experiments. The EDXRD investigations were performed at HASYLAB, beamline F3 at DESY in Hamburg, Germany. White synchrotron radiation was used in combination with a germanium detector system cooled with liquid nitrogen. The detector angle was set to approximately 2° and the collimator to 0.2 × 0.2 mm^2. The reactions were carried out in Schott Duran glass culture tubes (5 mL) placed in a custom-made reactor system heated by an external thermostat to 130 °C.[31] To investigate the formation of **2** and **3** the optimized reaction conditions established form the HT experiments were chosen. The starting materials were employed as aqueous solutions (for **2**, 200 μL 2 M APPA, 650 μL 2 M $Zn(NO_3)_2\cdot 6H_2O$, 1 mL water, and 150 μL 4 M NaOH; for **3**, 200 μL 2 M APPA, 100 μL 2 M $Zn(NO_3)_2\cdot 6H_2O$, 600 μL water, and 100 μL 4 M NaOH) and were homogenized by stirring during the reaction. Due to the fact that the formation of **2** and **3** takes place at the same molar ratio Zn^{2+}/APPA, but with different amounts of NaOH, the phase transformation of **2** into **3** was also investigated. The starting materials were employed as used for the formation of **2**, and after 360 s the reaction was interrupted to add 100 μL of 4 M NaOH in 1 mL of water. After 30 min the reaction was stopped again, and 280 μL of 2 M HNO_3 was added. Using a syringe, the base and acid were added through a septum in the cap of the glass tube. The measurement time for each EDXRD spectrum was 45 s for the formation of

dx.doi.org/10.1021/ic202589s | Inorg. Chem. 2012, 51, 3108–3118

Table 2. Summary of Crystal Data and Refined Structure Parameters for $[Zn(O_3P-C_3H_6-NH_2)]\cdot H_2O$ (3), $Zn(O_3P-C_3H_6-NH_3)(NO_3)(H_2O)$ (4), $Zn(O_3P-C_4H_8-NH_2)$ (5), and $Zn(O_3P-C_4H_8-NH_3)(NO_3)(H_2O)$ (6)[a]

	compound 3	compound 4	compound 5	compound 6
formula	$C_3H_{10}O_4PNZn$	$C_3H_{11}O_7PN_2Zn$	$C_4H_{10}O_3PNZn$	$C_4H_{13}O_7PN_2Zn$
fw (g/mol)	220.47	661.06	216.48	297.51
cryst syst	monoclinic	monoclinic	monoclinic	monoclinic
space group	$P2_1/c$ (No. 14)	$P2_1/c$ (No. 14)	$P2_1/c$ (No. 14)	Cc (No. 9)
a, b, c (Å)	9.094(2)	15.628(4)	8.570(7)	4.783(7)
	5.0118(7)	17.013(3)	8.378(4)	38.43(3)
	16.067(4)	10.544(2)	9.902(6)	5.948(8)
β (deg)	90.38(2)	103.78(1)	90.94(5)	91.44(5)
V (Å^3)	732.3(2)	2701.1(4)	710.9(8)	1043.6(3)
Z	4	8	4	4
R_{wp}	0.0625	0.0599	0.0576	0.0493
R_{exp}	0.0331	0.0149	0.0358	0.0251
R_{bragg}	0.0302		0.0159	
GOF	1.888	3.998	1.609	1.96

[a]Rietveld refinements were carried out for compounds **3** and **5**. The results of the Pawley fits are given for compounds **4** and **6**.

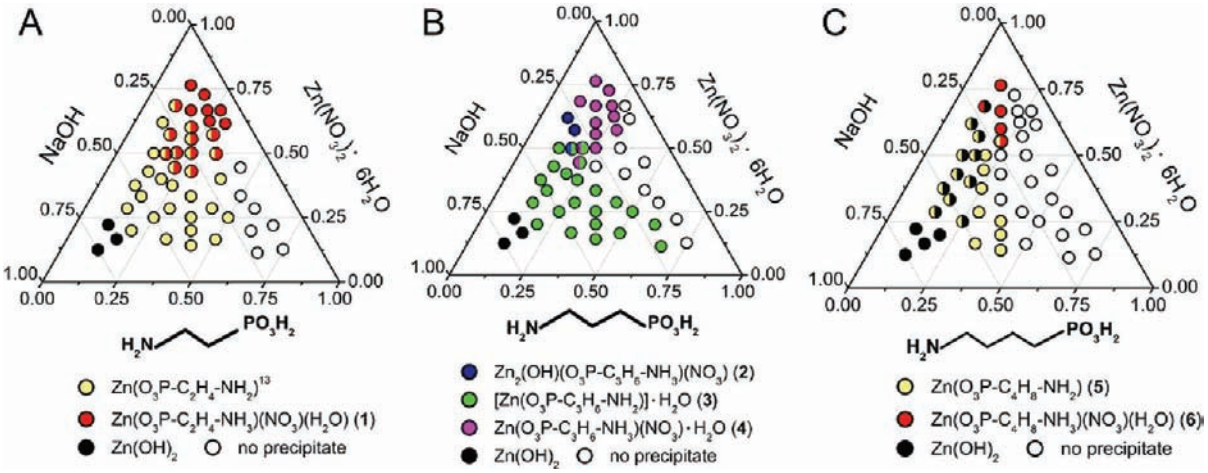

Figure 1. Crystallization diagrams of the system $Zn(NO_3)_2\cdot 6H_2O$/AAPA/NaOH at 130 °C.

compound **2** and the transformation as well as 60 s for the formation of compound **3**.

RESULTS AND DISCUSSION

HT Investigations. The HT experiments allow a systematic and fast investigation of complex reaction systems. One possibility to systematically study a reaction system is to vary stepwise the molar ratios of the starting materials. On the basis of the XRPD measurements of the resulting products a ternary crystallization diagram can be set up.[47,48] The diagrams of the systems $Zn(NO_3)_2\cdot 6H_2O$/AEPA/H_2O/NaOH, $Zn(NO_3)_2\cdot 6H_2O$/APPA/H_2O/NaOH, and $Zn(NO_3)_2\cdot 6H_2O$/ABPA/H_2O/NaOH are shown in Figure 1.

The ternary diagram **A** shows that in addition to $Zn(OH)_2$ two compounds can be observed. At the molar ratios Zn^{2+}/AEPA/NaOH = (0.33−6.5)/1/(0.5−4) (pH = 6−9) the literature known compound $Zn(O_3P-C_2H_4-NH_2)$[14] (Zn(AEPA)) was obtained. $Zn(O_3P-C_2H_4-NH_3)(NO_3)(H_2O)$ (**1**) was formed in a smaller field of formation under more acidic conditions (pH = 3−5). Here, a single crystal of **1** could be isolated at a molar ratio of 2/1/0.25. Some molar ratios [(1.5−6.5)/1/(0.5−2)] led to a mixture of both compounds. Using 3-aminopropylphosphonic acid (diagram B), three new compounds and $Zn(OH)_2$, under highly basic conditions (pH = 9−14), are obtained. Single-phase products of $Zn_2(OH)(O_3P-C_3H_6-NH_3)_2(NO_3)$ (**2**) are formed at the molar ratio Zn^{2+}/APPA/NaOH = 4/1/2 and 6.5/1/3 (pH = 5−6), while $[Zn(O_3P-C_3H_6-NH_2)]\cdot H_2O$ (**3**) is observed over a larger field of formation under more alkaline conditions (pH = 6−8) at molar ratios (0.17−4)/1/(0.33−4). A single crystal of **2** was isolated employing the molar ratio 6.5/1/3. The XRPD pattern used for the crystal structure determination of **3** was performed with the microcrystalline powder obtained at the molar ratio of 1/1/2. A third product $Zn(O_3P-C_3H_6-NH_3)(NO_3)(H_2O)$ (**4**) was isolated in the higher acidic region (pH = 4−5). The molar ratio 3/1/0.5 led to a well crystalline product of **4** which was used for the determination of the lattice parameters and the Pawley fit (Figure S3). Only three molar ratios (3/1/2, 2.5/1/1.5, and 2: 1: 1.5) resulted in mixtures of **2**/**3** and **3**/**4**, respectively. In some cases, no precipitate was found. Results of the investigation using 3-aminobutylphosphonic acid are presented in diagram C. As observed in diagram A two new phases in addition to $Zn(OH)_2$ are found. At pH values in the range pH = 6−7 [Zn^{2+}/ABPA/NaOH = (0.33−2)/1/(1−1.5)], the single-phase product $Zn(O_3P-C_4H_8-NH_2)$ (**5**) is obtained. Product **5** obtained by employing the molar ratio 0.5/1/1.5 was used for the structure determination from XRPD data. Smaller linker molecule concentrations result in a mixture

dx.doi.org/10.1021/ic202589s | Inorg. Chem. 2012, 51, 3108−3118

of **5** and $Zn(OH)_2$. $Zn(O_3P{-}C_4H_8{-}NH_3)(NO_3)(H_2O)$ (**6**) is formed in a small field of formation corresponding to molar ratios (3−6.5)/1/1 (pH = 5). XRPD pattern used for the determination of the lattice parameters and the Pawley fit of **6** was performed with the microcrystalline powder obtained from the microwave synthesis, due to the higher crystallinity of the product. Compared to system A and B, in a large area of the crystallization diagram [molar ratios (0.17−4)/1/(0.17−1)], no precipitates were formed.

Crystal Structure of $Zn(O_3P{-}C_2H_4{-}NH_3)(NO_3)(H_2O)$ (1). Compound **1** has previously been mentioned in the literature, but no crystal structure was reported.[49] We were able to determine the crystal structure using single crystal X-ray diffraction data. The layered structure of compound **1** consists of Zn^{2+} and 2-ammoniumethylphosphonate $(O_3P{-}C_2H_4{-}NH_3)^-$ ions as well as one water molecule and one nitrate ion in the asymmetric unit. The Zn^{2+} ions are 6-fold coordinated by oxygen atoms. Each metal ion is connected to four $(O_3P{-}C_2H_4{-}NH_3)^-$ ions via five P−O−Zn bonds. The coordination sphere is completed by one coordinated water molecule (OW) (Figure 2), that forms hydrogen bonds with the oxygen atoms of neighboring phosphonate group (O1, O2, O3). Corner-linked ZnO_6-polyhedra are observed that form layers in the *a*,*c*-plane (Figure 3, left). This coordination geometry is very similar to that observed for $M(O_3PC_6H_5)$ (M = Mg, Mn, Zn, Ca, Cd)[16] and $M_2(O_3PCH_2C_6H_4CH_2PO_3)\cdot 2H_2O$ (M = Mn, Ni, Cd).[50] Along the *b*-axis, the alkylammonium $-C_2H_4-NH_3^+$ and the nitrate ions are connected via N−H···O hydrogen bonds (Figure 3, right). Selected bond lengths and angles as well as the hydrogen bonding scheme are given in Tables S7 and S8 in the Supporting Information.

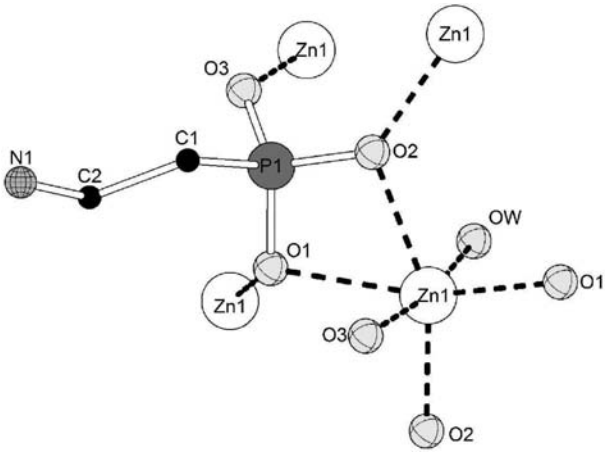

Figure 2. Coordination sphere of the Zn^{2+} ion in compound **1**. H-atoms are omitted for clarity.

Crystal Structure of $Zn_2(OH)(O_3P{-}C_3H_6{-}NH_3)_2(NO_3)$ (2). Compound **2** crystallizes in colorless thin needles and was obtained at pH = 4−5 compared to **1** which was obtained at pH = 3−5 and also contains a protonated amino group. The framework is composed of Zn^{2+} and 3-ammoniumpropylphosphonate ions as well as hydroxide and nitrate ions. The Zn^{2+} ion is connected to three $(O_3P{-}C_3H_6{-}NH_3)^-$ ions and one hydroxide ion to form ZnO_4-polyhedra. Each hydroxide oxygen atom (O4) connects two zinc atoms (Figure 4), and dimeric Zn_2O_7 clusters are formed (Figure 5, left).

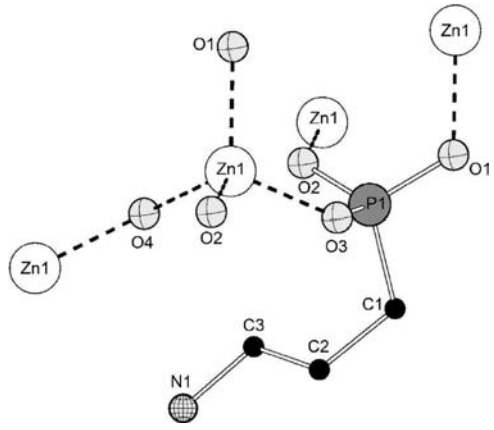

Figure 4. Coordination environment of Zn^{2+} and the phosphonate group in compound **2**. H-atoms have been omitted for clarity.

The oxygen atoms of the phosphonate group (O1, O2, O3) act as bridging ligand atoms to connect the corner-sharing tetrahedra in the *b*,*c*-plane. In contrast to compound **1**, the

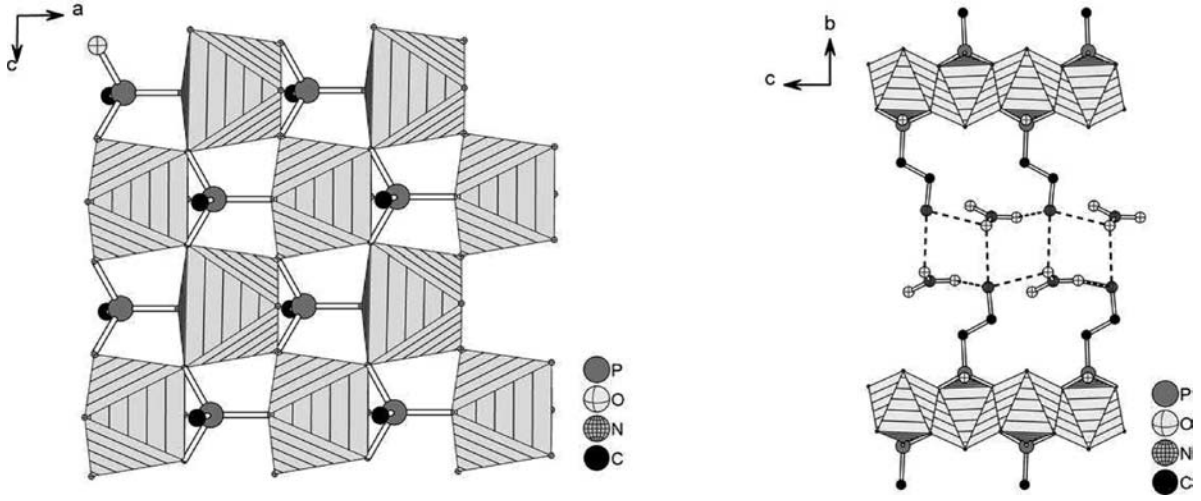

Figure 3. Left panel shows the layer of corner-sharing ZnO_6-polyhedra (shaded in gray) in the *a*,*c*-plane. Right panel shows the $-C_2H_4NH_3^+$-groups of the linker molecules pointing into the interlayer space (along the *b*-axis). Hydrogen bonds between the $-NH_3^+$ and the NO_3^- ions are observed (dotted lines). For clarity hydrogen atoms are omitted.

dx.doi.org/10.1021/ic202589s | *Inorg. Chem.* 2012, 51, 3108−3118

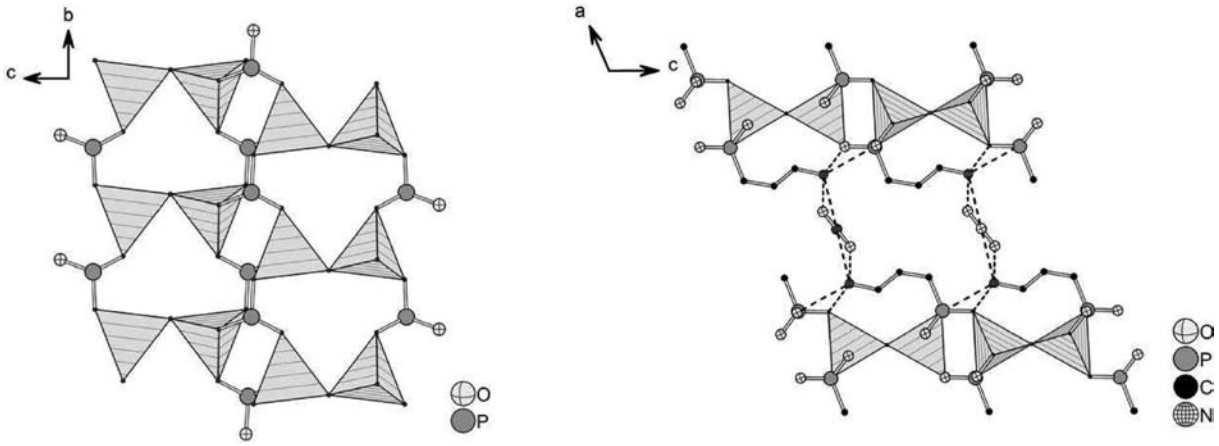

Figure 5. Left panel shows corner-sharing ZnO_4-polyhedra form Zn_2O_7 clusters (shaded in gray), which are connected by phosphonate groups in the *b*,*c*-plane in **2**. Right panel shows that the $C_3H_6NH_3^+$-groups of the linker molecule are involved in the formation of intralayer H-bonds and the interconnection of the layers is accomplished via H-bonds with the NO_3^- ions (dotted lines). For clarity hydrogen atoms are not drawn.

propylammonium group $-C_3H_4-NH_3^+$ does not protrude perpendicular into the interlayer space. Instead, intralayer N−H···O−P H-bonds are formed that stabilize the structure, and N−H···O−N hydrogen bonds lead to the interconnection of the layers (Figure 5, right). Selected bond lengths, angles, and the hydrogen bonding scheme are given in Tables S9 and S10 in the Supporting Information.

Crystal Structure of $[Zn(O_3P-C_3H_6-NH_2)]\cdot H_2O$ (3). The crystal structure of **3** was obtained from XRPD data. The final Rietveld plot is shown in Figure 6.

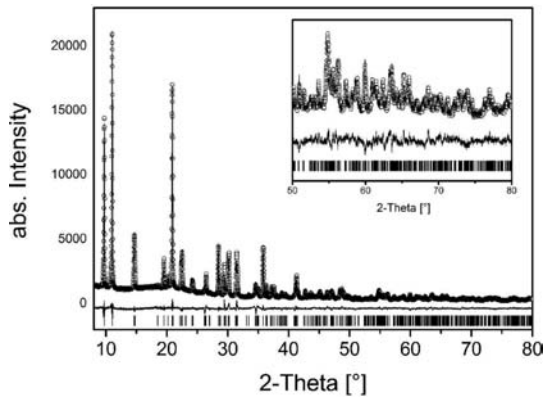

Figure 6. Observed (○) and calculated (—) XRPD pattern of the Rietveld refinement of compound **3**. The vertical lines below the patterns indicate the Bragg positions, and the bottom curve represents the difference plot of the measured vs calculated pattern.

In comparison to compound **2** (formed at pH = 4−5), the second Zn-APPA-compound **3** is obtained at pH = 6−8 and exhibits a framework containing one Zn^{2+}, one $(O_3P-C_3H_6-NH_2)^{2-}$ ion, and one water molecule in the asymmetric unit. The zinc ions are surrounded by three oxygen atoms and one nitrogen atom from four different 3-aminopropylphosphonate ions, and ZnO_3N-polyhedra are formed (Figure 7).

Corner-sharing CPO_3- and ZnO_3N-polyhedra lead to the formation of double chains along the *b*-axis which are connected by the C_3H_6-groups to build layers in the *a*,*b*-plane (Figure 8, left). Water molecules (OW) are located between the layers, and hydrogen bonds can be anticipated that lead to an interconnection of the layers (Figure 8, right). Selected bond lengths and angles as

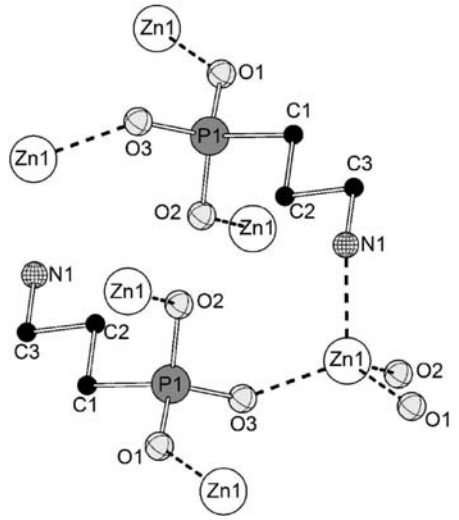

Figure 7. Coordination environment of Zn^{2+} and the phosphonate group in compound **3**. H-atoms are omitted for clarity.

well as the anticipated lengths of the hydrogen bonds are given in Tables S11 and S12 in the Supporting Information.

Crystal Structure of $Zn(O_3P-C_4H_8-NH_2)$ (5). The crystal structure of **5** was obtained from XRPD data. The final Rietveld plot is shown in Figure 9.

Employing 4-aminobutylphosphonic acid instead of the 2-aminoethylphoshonic acid compound **5** which is isoreticular to Zn(AEPA)[14] is obtained. The framework of $Zn(O_3P-C_4H_8-NH_2)$ contains one Zn^{2+} and one $(O_3P-C_4H_8-NH_2)^{2-}$ ion in the asymmetric unit as observed for **3**. Each Zn^{2+} ion is surrounded by three oxygen atoms and one nitrogen atom to form ZnO_3N-polyhedra. Every zinc atom is also connected to four linker molecules (Figure 10).

The coordination environment of the zinc ion in compound **5** is very similar to the one observed in compound **3** (Figure 7). In contrast to **3**, corner-sharing of CPO_3- and ZnO_3N-polyhedra leads to the formation of layers containing 4- and 8-rings (Figure 11, left). These layers are connected by the organic C_4H_8-unit, which leads to a three-dimensional pillared framework (Figure 11, right). Selected bond lengths and angles are given in Table S13 in the Supporting Information.

dx.doi.org/10.1021/ic202589s | *Inorg. Chem.* 2012, 51, 3108−3118

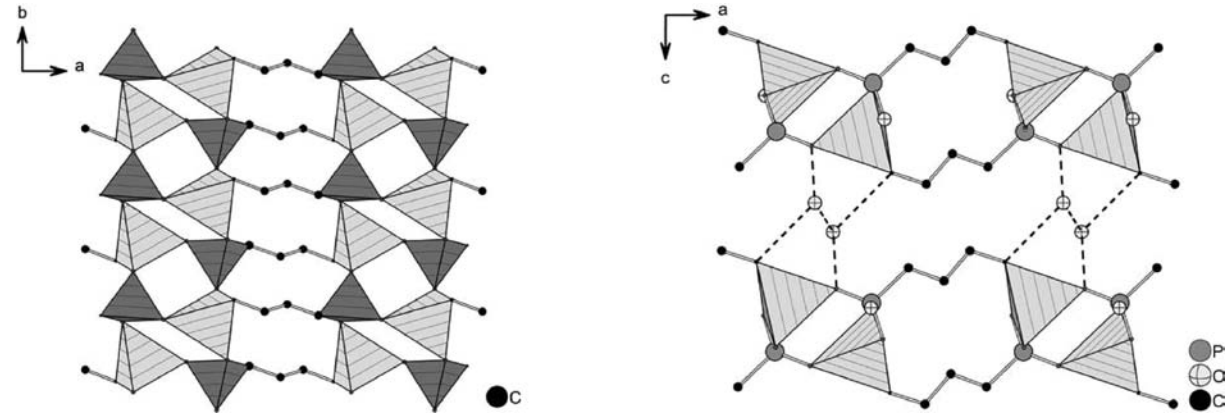

Figure 8. Left panel shows ZnO_3N- (shaded in light gray) and CPO_3-polyhedra (shaded in dark gray) which form double chains in compound **3** that are connected via the C_3H_6-groups of the linker molecule in the *a*,*b*-plane. Right panel shows water molecules located between the layers and hydrogen bonds which can be anticipated (dotted lines) that lead to the interconnection of the layers.

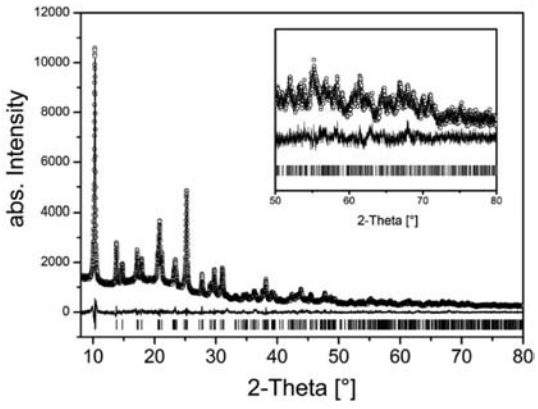

Figure 9. Observed (○) and calculated (—) XRPD pattern of the Rietveld refinement of compound **5**. The vertical lines below the patterns indicate the Bragg positions, and the bottom curve represents the difference plot of the measured vs calculated pattern.

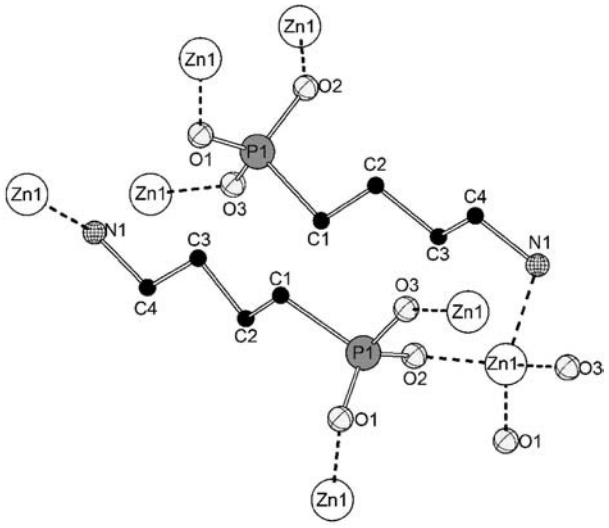

Figure 10. Coordination environment of Zn^{2+} ions and the phosphonate group in compound **5**.

Crystal Structure of $Zn(O_3P–C_4H_8–NH_3)(NO_3)(H_2O)$ (6). On the basis of the established composition and the refined lattice parameters the structure model of **6** was calculated using structure information of **1** ($Zn(O_3P–C_2H_4–NH_3)(NO_3)(H_2O)$).

On the basis of the characterization results, compound **6** was assumed to be isoreticular to compound **1**. Thus, using structure simulation by applying force field methods as implemented in Materials Studio,[46] a structural model could be obtained. Although we were not able to carry out a Rietveld refinement due to the inferior quality of the XRPD pattern, the comparison of the calculated and the measured XRPD patterns agree reasonably well (Figure 12, the Pawley fit obtained from XRPD data of **6** is shown in Figure S4). The bond lengths and angles from the model are in the range of the values observed for **1** (Table S14). Thus, the corner-linked ZnO_6-polyhedra form layers in the *a*,*c*-plane. Along the *b*-axis, the alkylammonium $–C_4H_8–NH_3^+$ and the nitrate ions are connected via anticipated hydrogen bonds. Since the structure of **6** is isoreticular to the one of **1**, only the separation of the inorganic layers increases from 1467.1(6) to 1921(3) pm.

$Zn(O_3P–C_3H_6–NH_3)(NO_3)(H_2O)$ (4). Compound **4** was obtained under more acidic conditions (pH = 4–5) compared to compounds **2** and **3**. A well crystallized product was used to determine the lattice parameter from synchrotron data measured at the DESY Hamburg, HASYLAB, beamline G3 (monoclinic, a = 15.628(4) Å, b = 17.013(3) Å, c = 10.544(2) Å, β = 103.78(1)°, V = 2701.1(4) Å^3, FOM = 28.6, spacegroup $P2_1/c$). It was not possible to determine the crystall strucuture until now. The measured powder diffraction pattern and the reflection positions as well as a Pawley fit are shown in Figure S3. The composition of **4** was determined to be $Zn(O_3P–C_3H_6–NH_3)(NO_3)(H_2O)$ on the basis of infrared spectroscopy, elemental analysis, and thermogravimetric investigations.

IR and Raman Spectroscopy Study. The title compounds were studied by infrared and Raman spectroscopy (Figures S5–S10). All compounds show the typical bands for the P–C and P–O stretching vibrations of the CPO_3-group in the region 1130–950 cm^{-1}. Specific vibration bands due to the presence of characteristic groups are listed in Table 3. These confirm the structural results and the composition of the title compounds **1**–**6**.

Thermal Study. Thermogravimetric (TG) measurements up to 900 K in air using a heating rate of 2 K/min were performed to gain deeper insight into the thermal stability of the compounds. The TG curves of compounds **1**–**6** are shown in Figures S11–S16, and the results of the evaluation are listed in Table 4. The TG curves of compounds **1**, **3**, **4**, and **6** show a

dx.doi.org/10.1021/ic202589s | *Inorg. Chem.* 2012, 51, 3108–3118

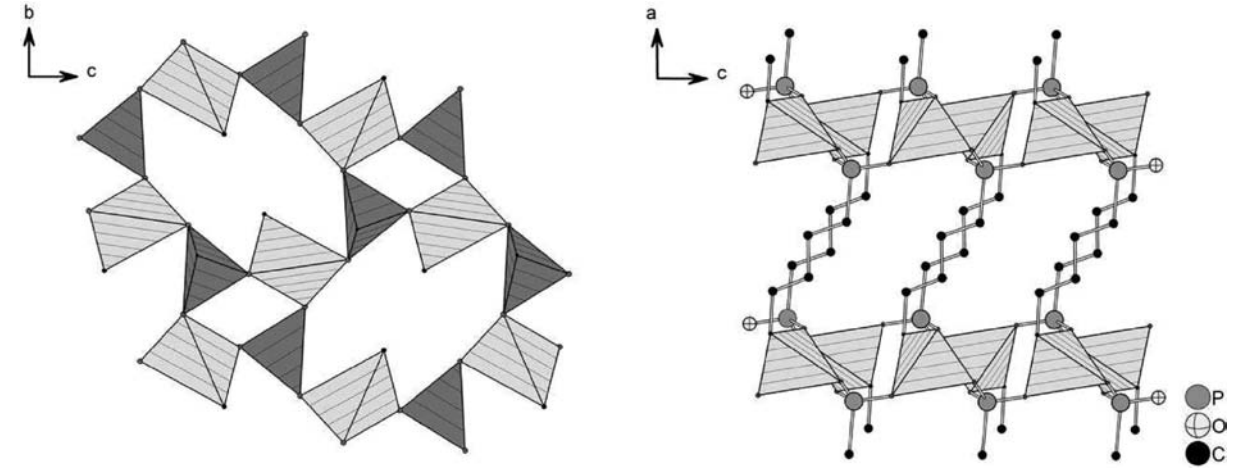

Figure 11. Left panel shows layers of ZnO_3N- (shaded in light gray) and CPO_3-polyhedra (shaded in dark gray) containing 4- and 8-rings in the *b*,*c*-plane in compound **5**. Right panel shows that the layers are connected via the C_4H_8-groups along the *a*-axis, which leads to a three-dimensional pillared framework.

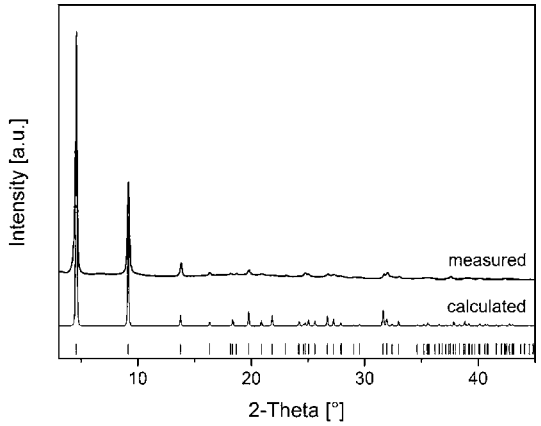

Figure 12. Comparison of the calculated and the measured XRPD patterns of compound **6**.

weight loss in the range 60−140 °C. These steps are dedicated to the loss of one water molecule per formula unit confirmed by the good agreement of observed and calculated weight losses. Above 200 °C the decomposition of the organic molecule as well as the nitrate ion (**1**, **4**, and **6**) takes place. The decomposition of compounds **2** and **5** starts at 140 and 60 °C, respectively. All TG curve results show a multistep decomposition which is completed in a range 760−840 °C.

Discussion. With the high-throughput methodology, a variety of new compounds were discovered, which allows the extraction of reaction trends and the comparison of the structural data (Figure 13).

While an even number of carbon atoms n = 2, 4 led to two compounds in each case, an odd number n = 3 led to three new different compounds. The compounds containing an even number of carbon atoms are isoreticular. The use of AEPA led to one new compound $Zn(O_3P{-}C_2H_4{-}NH_3)(NO_3)(H_2O)$ (**1**) and the literature known compound $Zn(O_3P{-}C_2H_4{-}NH_2)$.[14] Elongation of the ethyl linker chain by one $-CH_2-$ group resulted in three new compounds: $Zn_2(OH)(O_3P{-}C_3H_6{-}NH_3)_2(NO_3)$ (**2**), $[Zn(O_3P{-}C_3H_6{-}NH_2)]{\cdot}H_2O$ (**3**), and $Zn(O_3P{-}C_3H_6{-}NH_3)(NO_3)(H_2O)$ (**4**). The formation of the compounds of each system strongly depends on the pH-value of the reaction mixture. While **1** is formed at pH = 3−5 and contains $-NH_3^+$ groups and nitrate ions, the deprotonated linker in $Zn(O_3P{-}C_2H_4{-}NH_2)$[14] is observed at pH = 6−9. Using APPA, compound **2** is obtained in the range pH = 5−6. Although $-NH_3^+$ groups are observed in **2** and it is obtained under mildly acidic conditions, it also contains bridging hydroxide ions. While **2** is observed in a very small field of formation, **3** is obtained under more basic conditions (pH = 6−8) in a larger field of formation. As expected, the amino group is not protonated, and also, no hydroxide ions are incorporated. Compound **4**, which is formed at more acidic conditions (pH = 4−5) compared to **2** and **3**, contains only the $-NH_3^+$ group and NO_3^- ions for charge balance. Employing ABPA, compounds **5** and **6** which are isoreticular to $Zn(O_3P{-}C_2H_4{-}NH_2)$[14] and **1** are formed. The pH-values of the formation of **5** (pH = 6−7) and **6** (pH = 5) correspond well to those for the formation of $Zn(O_3P{-}C_2H_4{-}NH_2)$[14] and **1**. In summary, a protonated amino group is obtained at pH < 6.

Table 3. Specific Vibration Bands of $Zn(O_3P{-}C_2H_4{-}NH_3)(NO_3)(H_2O)$ (1), $Zn_2(OH)(O_3P{-}C_3H_6{-}NH_3)_2(NO_3)$ (2), $[Zn(O_3P{-}C_3H_6{-}NH_2)]{\cdot}H_2O$ (3), $Zn(O_3P{-}C_3H_6{-}NH_3)(NO_3)(H_2O)$ (4), $Zn(O_3P{-}C_4H_8{-}NH_2)$ (5), and $Zn(O_3P{-}C_4H_8{-}NH_3)(NO_3)(H_2O)$ (6)

	functional groups and wavenumbers [cm^{-1}]					
	(μ-OH)	H_2O	NH_3^+	NH_2	CH_2	NO_3
1		3446, ν	3145−3053, ν		2970, ν_{as}	1575, ν_{as}
		1623, δ	1518, δ_s		1465, δ	1300, ν_s
2	3596, ν		3200−3120, ν		2935, ν_{as}	1580, ν_{as}
	1625, δ		1517, δ_s		2880, ν_s	1288, ν_s
					1470, δ	
3		3480, ν		3278, ν_{as}	2942, ν_{as}	
		1630, δ		3150, ν_s	2883, ν_s	
				1597, δ	1482, δ	
4		3400, ν	3146−3019, ν		2949, ν_{as}	1541, ν_{as}
		1620, δ	1525, δ_s		2873, ν_s	1311, ν_s
					1467, δ	
5				3287, ν_{as}	2942, ν_{as}	
				3173, ν_s	2886, ν_s	
				1597, δ	1478, δ	
6		3442, ν	3151−3060, ν		2940, ν_{as}	1580, ν_{as}
		1620, δ	1520, δ_s		2869, ν_s	1313, ν_s
					1470, δ	

dx.doi.org/10.1021/ic202589s | *Inorg. Chem.* 2012, 51, 3108−3118

Table 4. Results of the Thermogravimetric Investigation of $Zn(O_3P-C_2H_4-NH_3)(NO_3)(H_2O)$ (1), $Zn_2(OH)(O_3P-C_3H_6-NH_3)_2(NO_3)$ (2), $[Zn(O_3P-C_3H_6-NH_2)]\cdot H_2O$ (3), $Zn(O_3P-C_3H_6-NH_3)(NO_3)(H_2O)$ (4), $Zn(O_3P-C_4H_8-NH_2)$ (5), and $Zn(O_3P-C_4H_8-NH_3)(NO_3)(H_2O)$ (6)

			weight loss dedicated to dehydration and total weight loss [%]		
compound	water molecule	temperature range of dehydration and total weight loss [%]	obsd	calcd	product
1	1	60−130	7.0	6.7	X-ray amorphous
		75−780	48.6	46.4	
2					$Zn_2P_2O_7$
		140−840	40.3	40.1	
3	1	60−145	7.5	8.1	$Zn_2P_2O_7$
		60−840	33.8	34.0	
4	1	60−140	6.3	6.3	X-ray amorphous
		60−780	47.4	49.0	
5					$Zn_2P_2O_7$
		60−780	35.5	33.3	
6	1	55−115	6.0	6.1	$Zn_2P_2O_7$
		55−760	52.3	51.4	

[a]Determined by XRPD measurements.

The most profound difference between the structures obtained using aminoalkylphosphonic acids $H_2O_3P-C_nH_{2n}-NH_2$ ($n = 2 - 4$) with $n = 2$, 4 and $n = 3$ is the arrangement of the alkyl chain in relation to the zinc phosphonate layers. For $n = 2$ and 4 the alkyl chains are in all structures perpendicular to the layers. As reported for $Co(O_3PC_2H_4NH_2)$[20] in ZnAEPA[14] and **5**, the $-NH_2$ groups take part in the coordination of the Zn^{2+} ions, and ZnO_3N polyhedra are formed. In the case of the protonation of the $-NH_2$ group, the coordination environment of the Zn^{2+} ions is expanded to 6-fold coordination involving O-atoms of the phosphonate groups and one water molecule each. The $-NH_3^+$ groups are involved in hydrogen bonds with the NO_3^- ions leading to the interconnection of the layers. With $n = 3$ the alkyl chains are aligned parallel to the zinc phosphonate layers. In the case of the $-NH_2$ group not being protonated, intralayer coordination and formation of ZnO_3N polyhedra is observed (**3**). The protonation of the amino group leads to a structure containing ZnO_4 polyhedra, and the $-NH_3^+$ group is involved in the formation of intralayer H-bonds and H-bonds to NO_3^- ions leading to the interconnection of the layers.

In Situ EDXRD Investigation. Results from HT, scale-up, and MW-assisted heating investigations have shown that the scale-up synthesis under stirring conditions of compounds **2** and **3** led to very crystalline products. Therefore, the formation of **2** and **3** was also investigated by in situ EDXRD measurements. The formation of compound **2** and compound **3** was studied using conventional heating at a temperature of 130 °C. For an evaluation of the data, the reaction progress $\alpha(t) = I(t)/I(t_\infty)$ was determined, where I is the intensity at a given time t and at the end of the reaction t_∞, respectively. The intensity I was obtained by integrating the 100 reflection of **2** and the 200 reflection of **3** (maximal error 2.5% and 6% for **2** and **3**, respectively). The results of the time-dependent EDXRD measurements (surface plot) and the resulting normalized integrals $\alpha(t)$ are shown in Figure 14. For compound **2** one signal is observed for the first time after 90 s at 27 keV, which corresponds to the 100 reflection at 7.9° (2θ) in the XRPD measurement. After 230 s the intensity reaches a maximum. For compound **3** two signals are observed for the first time after

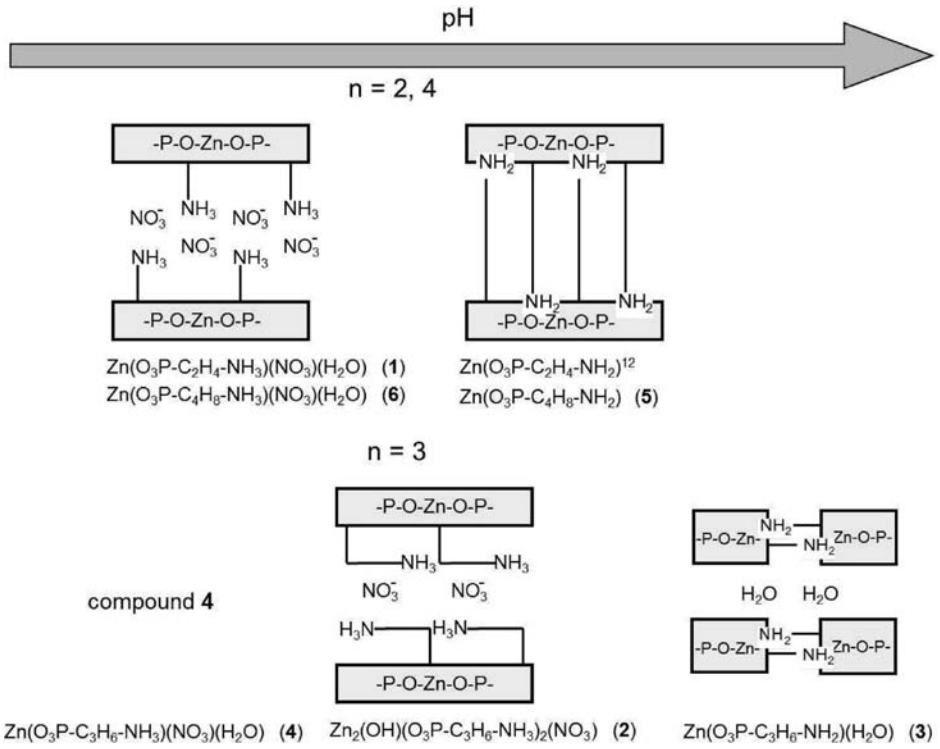

Figure 13. Schematic illustration of the influence of the alkyl chain length and the pH value on the formation of the title compounds.

dx.doi.org/10.1021/ic202589s | Inorg. Chem. 2012, 51, 3108−3118

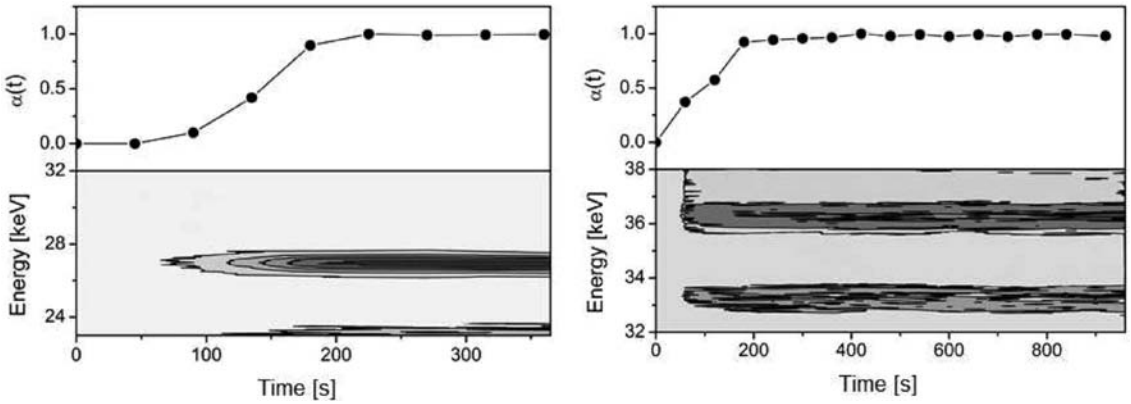

Figure 14. Surface plot and reaction progress ($\alpha(t)$) of the formation of compound **2** (left) and compound **3** (right) studied by in situ EDXRD measurements.

60 s at 33.5 and 36.5 keV which correspond to the 100 and 200 reflections at 9.7° and 11.0° (2θ) in the XRPD measurement. After approximately 200 s the intensities reach a maximum.

According to Figure 14, only very short reaction times (ca. 200 s) are necessary to obtain fully crystallized products **2** and **3**. Since compound **2** contains a protonated amino group which does not coordinate to the Zn^{2+} ion the possible phase transformation to compound **3** (Figure 15) was investigated.

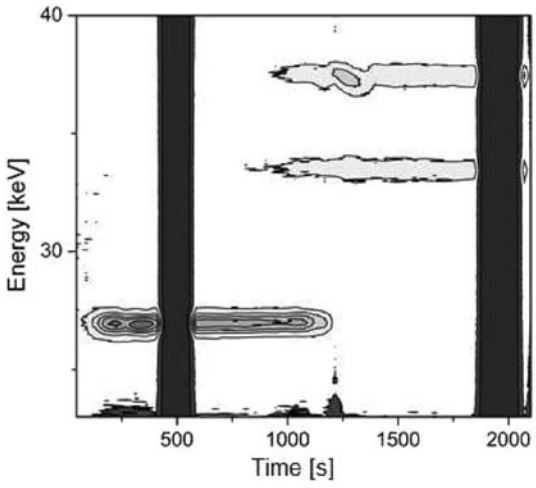

Figure 15. Surface plot of the EDXRD experiments of the phase transformation of **2** into **3**. After 360 s NaOH was added. After 1800 s HNO_3 was added. Addition of NaOH led to the transformation of **2** into compound **3**, while addition of HNO_3 led to the dissolution of **3**. The dark bars indicate the addition of the NaOH and HNO_3.

After full crystallization of **2**, the addition of NaOH leads to a decrease of the signal intensity at 27 keV, and the two signals at 34 and 37 keV develop simultaneously. After several minutes, compound **2** was completely transformed into compound **3**. The following addition of nitric acid leads only to the dissolution of the reaction product.

CONCLUSION

With the HT methodology six new zinc aminoalkylphosphonates were discovered, and their fields of formation were established. Employing various methods to determine the crystal structures, such as the structure determination from single crystal and powder XRD data as well as force field methods, we were able to establish synthesis−structure and ligand length−structure relationships. In situ EDXRD measurements showed that only very short reaction times are necessary for the formation of **2** and **3**, and that a phase transformation takes place upon variation of the pH (**2** → **3**).

ASSOCIATED CONTENT

Supporting Information

Additional reaction and characterization details. This material is available free of charge via the Internet at http://pubs.acs.org.

AUTHOR INFORMATION

Corresponding Author

*E-mail: stock@ac.uni-kiel.de. Phone: +49-431-880-1675. Fax: +49-431-880-1775.

ACKNOWLEDGMENTS

The allocated beamtime at HASYLAB, Hamburg, and the financial support by the DFG (Project STO 643/2) is gratefully acknowledged. We thank Inke Jess and Christian Näther for single crystal measurements, Mark Feyand for the support in the structure determinations from XRPD data and the EDXRD studies, Uschi Cornelissen and Stephanie Pehlke for spectroscopic measurements, Beatrix Seidlhofer for TG/DTA measurements, and the group of Prof. Dr. Wolfgang Bensch for the allocation of the reactor system for the in situ EDXRD studies

REFERENCES

(1) Clearfield, A. *Prog. Inorg. Chem.* **1998**, *47*, 371−510.
(2) Czaja, A. U.; Trukhan, N.; Müller, U. *Chem. Soc. Rev.* **2009**, *38*, 1284−1293.
(3) Kitagawa, S.; Kitaura, R.; Noro, S.-I. *Angew. Chem., Int. Ed.* **2004**, *43*, 2334−2375.
(4) Stock, N.; Stoll, A.; Bein, T. *Microporous Mesoporous Mater.* **2004**, *69*, 65−69.
(5) Shimizu, G. K. H.; Vaidhyanathan, R.; Taylor, J. M. *Chem. Soc. Rev.* **2009**, *38*, 1430−1449.
(6) Gagnon, K. J.; Perry, H. P.; Clearfield, A. *Chem. Rev.* **2012**, *112*, 1034−1054.
(7) Rowsell, J. L. C.; Yaghi, O. M. *Microporous Mesoporous Mater.* **2004**, *73*, 3−14.
(8) Bauer, S.; Bein, T.; Stock, N. *J. Solid State Chem.* **2006**, *179*, 145−155.
(9) Bauer, S.; Bein, T.; Stock, N. *Inorg. Chem.* **2005**, *44*, 5882−5889.
(10) Stock, N.; Frey, S. A.; Stucky, G. D.; Cheetham, A. K. *Dalton Trans.* **2000**, 4292−4296.

(11) Du, Z.-Y.; Xu, H.-B.; Li, X.-L.; Mao, J.-G. *Eur. J. Inorg. Chem.* **2007**, 4520−4529.
(12) Sonnauer, A.; Feyand, M.; Stock, N. *Cryst. Growth Des.* **2008**, *9*, 586−592.
(13) Sonnauer, A.; Stock, N. *J. Solid State Chem.* **2008**, *181*, 473−479.
(14) Drumel, S.; Janvier, P.; Deniaud, D.; Bujoli, B. *J. Chem. Soc., Chem. Commun.* **1995**, 1051−1052.
(15) Menke, A. G.; Walmsley, F. *Inorg. Chim. Acta* **1976**, *17*, 193−197.
(16) Cao, G.; Lee, H.; Lynch, V. M.; Mallouk, T. E. *Inorg. Chem.* **1988**, *27*, 2781−2785.
(17) Cao, G.; Lee, H.; Lynch, V. M.; Swinnea, J. S.; Mallouk, T. E. *Inorg. Chem.* **1990**, *29*, 2112−2117.
(18) Ouelette, W.; Yu, M. H.; O'Connor, C. J.; Zubieta, J. *Inorg. Chem.* **2006**, *45*, 3224−3239.
(19) Feyand, M.; Näther, C.; Rothkirch, A.; Stock, N. *Inorg. Chem.* **2010**, *49*, 11158−11163.
(20) Gemmill, W. R.; Smith, M. D.; Reisner, B. A. *J. Solid State Chem.* **2005**, *178*, 2658−2662.
(21) Drumel, S.; Janvier, P.; Bujoli-Doeuff, M.; Bujoli, B. *Inorg. Chem.* **1996**, *35*, 5786−5792.
(22) Bauer, E. M.; Bellitto, C.; Colaoietro, M.; Portalone, G.; Righini, G. *Inorg. Chem.* **2003**, *42*, 6345−6351.
(23) Fredoueil, F.; Massiot, D.; Janvier, P.; Gingl, F.; Bujoli-Doeuff, M.; Evain, M.; Clearfield, A.; Bujoli, B. *Inorg. Chem.* **1999**, *38*, 1831−1833.
(24) Rosenthal, G. L.; Caruso, J. *Inorg. Chem.* **1992**, *31*, 3104−3106.
(25) Zakowsky, N.; Wheatley, P. S.; Bull, I.; Attfield, M. P.; Morris, R. E. *Dalton Trans.* **2001**, 2899−2902.
(26) Samanamu, C. R.; Zamora, E. N.; Montchamp, J.-L.; Richards, A. F. *J. Solid State Chem.* **2008**, *181*, 1462−1471.
(27) Stock, N. *Microporous Mesoporous Mater.* **2010**, *129*, 287−295.
(28) Stock, N.; Bein, T. *Angew. Chem.* **2004**, *116*, 767−770.
(29) Bauer, S.; Stock, N. *Angew. Chem., Int. Ed.* **2007**, *46*, 6857−6860.
(30) Stock, N.; Bein, T. *J. Mater. Chem.* **2005**, *15*, 1384−1391.
(31) Engelke, L.; Schäfer, M.; Schur, M.; Bensch, W. *Chem. Mater.* **2001**, *13*, 1383−1390.
(32) Fisher, R. D.; Walton, R. I. *Dalton Trans.* **2009**, 8079−8086.
(33) Becker, H.; et al. *Organikum*, 22nd ed.; Wiley-VCH: Weinheim, 2004; p 600.
(34) Barycki, J.; Mastalerz, P.; Soroka, M. *Tetrahedron Lett.* **1970**, *36*, 3147−3150.
(35) Wasielewski, C.; Topolski, M.; Dembkowski, L. *J. Prakt. Chem.* **1989**, 507−509.
(36) Gali, H.; Prabhu, K. R.; Karra, S. R.; Katti, K. V. *J. Org. Chem.* **2000**, *65*, 676−680.
(37) Crabb, T. A.; Patel, A. *J. Chem. Soc., Perkin Trans.* **1985**, 191−195.
(38) McKenna, C. E.; Higa, M. T.; Cheung, N. H.; McKenna, M.-C. *Tetrahedron Lett.* **1977**, *2*, 155−158.
(39) Klinowski, J.; Almeida Paz, F. A.; Silva, P.; Rocha, J. *Dalton Trans.* **2011**, *40*, 321−330.
(40) *XRED version 1.19, X-Shape version 1.06, RECIPE, TWIN*; Stoe & Cie GmbH: Darmstadt, Germany, 1999.
(41) Burla, M. C.; Caliandro, R.; Camalli, M.; Carrozzini, B.; Cascarano, G. L.; De Caro, L.; Giacovazzo, C.; Polidori, G.; Siliqi, D.; Spagna, R. *J. Appl. Crystallogr.* **2007**, *40*, 609−613.
(42) Sheldrick, G. M. *SHELXTL-PLUS Crystallographic System*; Siemens Analytical X-ray Instruments Inc.: Madison,WI, 1992.
(43) Altomare, A.; Camalli, M.; Cuocci, C.; Giacovazzo, C.; Moliterni, A.; Rizzi, R. *J. Appl. Crystallogr.* **2009**, *42*, 1197−1202.
(44) *WinXPOW version 2.11*; Stoe & Cie GmbH: Darmstadt, Germany, 2005.
(45) Coelho, A. *Topas V4.1, Academic Version: General Profile and Structure Analysis Software for Powder Diffraction Data*; Bruker AXS Ltd.: Madison, WI, 2004.
(46) *Materials Studio 5.0*; Accelrys Inc.: San Diego, CA, 2008.
(47) Chamberlain, J. M.; Albrecht, T. A.; Sauvage, J. L. F.; Stern, C. L.; Poeppelmeier, K. R. *Cryst. Growth Des.* **2010**, *10*, 4868−4873.
(48) Francis, R. J.; Halasyamani, P. S.; Bee, J. S.; O'Hare, D. *J. Am. Chem. Soc.* **1999**, *121*, 1609−1610.
(49) Drumel, S.; Janvier, P.; Barboux, P.; Bujoli-Doeuff, M.; Bujoli, B. *Inorg. Chem.* **1995**, *34*, 148−156.
(50) Stock, N.; Bein, T. *J. Solid State. Chem.* **2002**, *167*, 330−336.